

Analysis of Enantioselective Biotransformations Using a Few Hundred Cells on an Integrated Microfluidic Chip

Karin M. Krone,[†] Rico Warias,[†] Cornelia Ritter,[‡] Aitao Li,^{‡,§} Carlos G. Acevedo-Rocha,^{‡,§} Manfred T. Reetz,^{*,‡,§} and Detlev Belder^{*,†}

[†]Institute of Analytical Chemistry, University of Leipzig, Linnéstrasse 3, 04103 Leipzig, Germany

[‡]Faculty of Chemistry, Philipps-Universität Marburg, Hans-Meerwein-Strasse, 35032 Marburg, Germany

[§]Max-Planck-Institut für Kohlenforschung, Kaiser-Wilhelm-Platz 1, 45470 Mülheim/Ruhr, Germany

Supporting Information

ABSTRACT: The investigation of stereoselective biocatalytic transformations at a single-cell level is to date an unsolved challenge. Here, we report the development of an integrated microfluidic device which enables the analytical characterization of enantioselective reactions at nanoliter scale by combining whole-cell catalyzed on-chip syntheses, chiral microchip electrophoresis, and label-free detection of enantiomers by deep UV time-resolved fluorescence. Using *Escherichia coli* expressing recombinant *Aspergillus niger* epoxide hydrolase as the model enzyme for various enantioselective reactions, we evaluated the approach for downscaling the reaction to a few hundred cells. Our work is thus an important step toward the analysis of single-cell stereoselective biocatalysis.

Lab-on-a-chip devices offer new possibilities to study and optimize chemical¹ and biochemical² processes at the micro- or nanoscale.³ This technology has become especially useful in bioanalytics⁴ and diagnostics⁵ where it can be combined with direct fluorescence-based readout techniques.⁶ Chip-based systems are also fascinating tools to study chemical reactions at high speed and with minimal sample consumption, as they can provide seamless integration of different functionalities.⁷ Even the integration of reaction and analysis of enantioselective transformations in a single separation setup are possible.^{8,9} For common synthetic organic reactions, however, this can be challenging, as sophisticated techniques have to be applied to analyze small molecules in complex reaction mixtures. In this context, the study of enantioselective catalysis is an especially demanding task because it requires the challenging differentiation of enantiomers.¹⁰

In a proof-of-concept study, we previously reported the integration of enantioselective biocatalysis and analysis on a single microchip.⁹ This was realized by combining a reaction structure for continuous flow synthesis with a separation channel for electrophoretic enantio-separation using *Aspergillus niger* epoxide hydrolase (ANEH) and mutants catalyzing the hydrolytic kinetic resolution of a racemic epoxide. The investigated reaction worked well with pure enzymes and cell lysates, but the disruption of cells and purification of proteins poses economical disadvantages. Indeed, industry usually prefers self-regenerating whole cells, because these can provide intracellular enzymes with

protection and stability, availability of protein cofactors for complex redox reactions, and physical coupling of multi-enzymatic reactions.¹¹

An additional advantage of using whole-cells is their suitability for high-throughput analysis for applications in synthetic organic chemistry and biotechnology. This is important when enzymes do not display a desired trait such as activity, stereoselectivity, or stability. To address this issue, directed evolution has emerged as a powerful protein engineering method, whereby enzymes are improved upon iterative cycles of gene mutagenesis, expression, and selection.¹² In a typical directed evolution experiment, “libraries” composed of thousands to millions of enzyme variants arising from single cells are generated. Some water-in-oil droplet-, vesicle-, or gel-shell bead-based microfluidic platforms have been developed to improve protein activity, binding, and stability,¹³ but devising such systems for engineering stereoselectivity is more challenging.¹⁴ The ideal screening-based directed evolution process requires low consumption of reagents, short screening and analysis time, as well as minimal employment of cells. Although some progress has been achieved in analyzing enantioselective reactions using single cells by conventional fluorescence-activated cell sorting (FACS),¹⁵ a prerequisite for this approach is to label the enantiomeric species differently to make them distinguishable. Moreover, such surrogates do not correspond to the “real” substrates used in practical applications.

Herein, we monitor various unlabeled enantiomers using whole cells as biocatalysts in an integrated reaction on a microfluidic device. A central aspect of our work is the evaluation of the minimal amount of cells required for enantioselective reactions and their analysis with the prospective aim to evaluate new avenues toward single-cell high-throughput enantioselective biocatalysis.

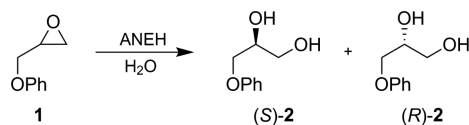
Our starting point is based on the previous on-chip model reaction of 1,2-epoxy-3-phenoxypropane (**1**) to form the product 3-phenoxy-1,2-propanediol (**2**) in a hydrolytic kinetic resolution by ANEH (Scheme 1),⁹ yielding two diol enantiomers (reaction stopping ideally at 50% conversion).

After optimizing the reaction conditions in classical reaction vessels and its analysis by capillary electrophoresis, we transferred the process to an integrated microfluidic fused-silica chip containing a flow reactor connected to a downstream electro-

Received: December 3, 2015

Published: January 29, 2016

Scheme 1. Enantioselective Model Reaction of 1,2-Epoxy-3-phenoxypropane (1) Hydrolysis Catalyzed by *A. niger* Epoxide Hydrolase (ANEH) To Form 3-Phenoxy-1,2-propanediol (2)



phoretic functional element with a crossing injection and separation channel (Figure 1a, in more detail Figure S1 of the Supporting Information (SI)).

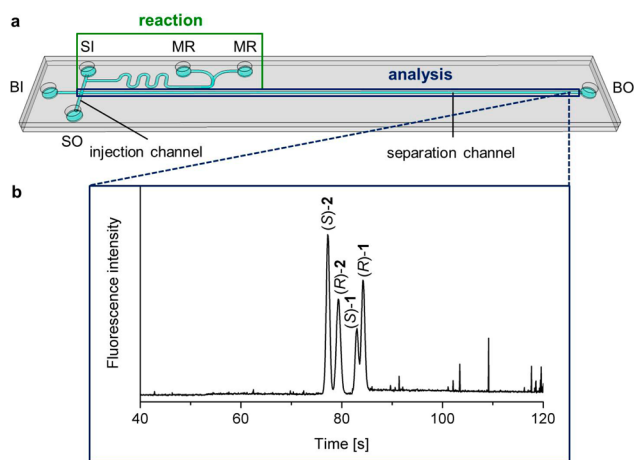


Figure 1. (a) Schematic drawing of the microfluidic chip with integrated functionalities: BI, buffer inlet vial; BO, buffer outlet vial; MR, microreactor vial; SI, sample inlet vial; SO, sample outlet vial. (b) Electropherogram after on-chip catalytic hydrolysis of 1 by *Escherichia coli* expressing ANEH-WT.

Upon assigning the peaks to the commercial substrate and product (Figure S2), a microbatch reaction was performed by pipetting 3.5 μL of 1 (40 $\mu\text{g}/\text{mL}$ in phosphate buffered saline (PBS)) and 3.5 μL of a cell suspension of *E. coli* BL21-Gold(DE3) (henceforth termed only as *E. coli*) expressing ANEH wild type (WT) (2.5×10^6 cells/ μL in PBS) into the sample inlet microcavity. The reaction mixture was separated by microchip electrophoresis (MCE) on the same device after a reaction time of 180 s. Enantiomers 1 and 2 were detected at the end of the separation channel by laser-induced deep UV-fluorescence (LIF). Figure 1b shows a typical result, which is in good agreement with our previous results where the reaction was performed in a chip with a different layout.⁹

As shown in Figure 1b, the two enantiomeric pairs of substrate 1 and product 2 are well separated in less than 90 s using highly sulfated β -cyclodextrin (15 mM) as chiral additive in the separation buffer (125 mM borate, pH 8.5). To verify that 1 hydrolysis was catalyzed by *E. coli* cells and not by free enzyme, the cells were removed. The corresponding supernatants derived from centrifugation as well as filtrates of the suspensions did not show any catalytic activity (Figure S6). Furthermore, it was verified that the monitored reaction was catalyzed by ANEH and not by native *E. coli* enzymes applying genetically unmodified *E. coli* (Figure S7).

An important aspect in the reaction downsizing is high detection sensitivity. Although single molecule detection is in principle possible by using fluorescence, this relies on bright fluorophores in the visible spectral range. However, the

achievable sensitivity in deep UV-fluorescence detection of unlabeled compounds is more challenging, especially for the intended on-the-fly detection during a fast electrophoretic separation. In contrast to our previous work,⁹ we now used a significantly advanced detection setup based on confocal microscopy, deep UV-fluorescence excitation (266 nm), and time correlated single photon counting (Figure S3). We investigated the achievable detection sensitivity and calculated the limits of detection (LODs) to be $\sim 1 \mu\text{M}$ for each enantiomer (signal-to-noise ratio (S/N) of 3; Figures S4 and S5). This is an improvement by a factor of 24 compared to previous work using a less performing detection system (Table S1). As the detection sensitivity is concentration-dependent, the obvious way to follow substrate conversion with a minimal amount of cells is to shrink down the reactor volume.

The initial reaction shown in Figure 1b was performed in a relatively large volume (7 μL) with high cell number (1.0×10^7 cells). To evaluate the minimal amount of cells needed to monitor conversions, the reaction volume was decreased stepwise by choosing different parts of the microfluidic channel network, as exemplified in Figure 2. The reaction time is an

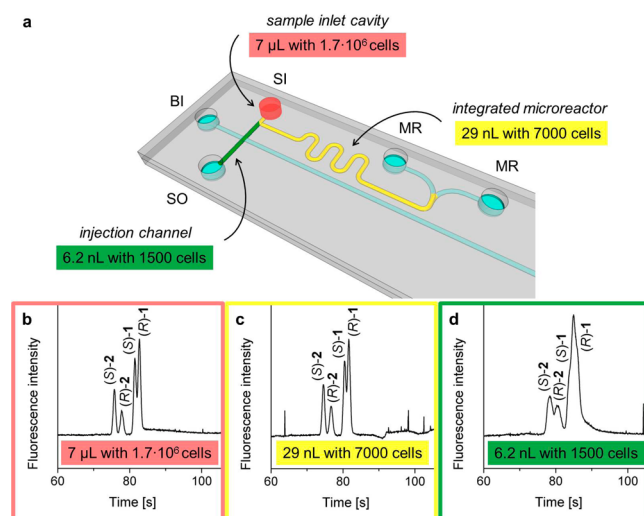


Figure 2. (a) Number of *E. coli* cells expressing ANEH-WT which are required for optimal performance of (S)-enantioselective whole-cell catalysis with the same substrate 1 concentrations in different reaction volumes on the microfluidic chip. (b) Typical electropherograms after on-chip catalytic hydrolysis by the respective number of cells.

important parameter and was optimized as well. While a longer reaction time leads to a higher conversion which facilitates the detection, it was found that with process times above 200 s sedimentation of the cells can complicate the flow due to occasional channel blockage. For this reason, a reaction time of 180 s was used as a compromise for the subsequent on-chip reactions.

To explore a possible downsizing of the reaction volumes, we performed reactions with 1:1 mixtures of substrate and cells (5.0×10^5 cells/ μL) in PBS either in the 7 μL inlet cavity, in the 29 nL integrated microreactor, or in the 6.2 nL injection channel (Figure 2). This corresponds to cell numbers of $(1.7 \pm 0.3) \times 10^6$, 7000 ± 1500 , or 1500 ± 300 , respectively. Representative data from MCE-LIF analysis is shown in Figure 2b–d. For all reaction volumes, the obtained analytical data, the reaction conversion, and sensitivity values (S/N 55 ± 9 ($n = 3$)) for the smallest signal (R)-2 are quite similar (Table S2). The reduced

separation resolution shown in Figure 2d can be explained by an imperfect injection as the injection channel is filled with reactants. Since good sensitivities were obtained, we further reduced cell number by a factor of 4. Respective data using concentrations down to 1.3×10^5 cells/ μL in the smallest reaction volume are shown in Figure 3. The S/N determined for

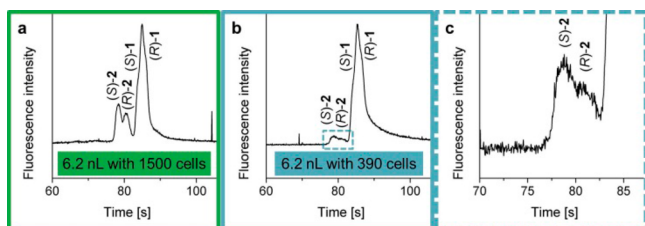


Figure 3. Low nanoliter scale enantioselective biocatalysis on the microfluidic chip. Electrophoretic data for on-chip (S)-enantioselective whole-cell catalysis with (a) 1500 and (b) 390 *E. coli* cells using a reaction volume of 6.2 nL; (c) enlargement of signal (S)-2 and (R)-2 from diagram (b).

the smallest signal ((R)-2) after catalysis with 390 cells is 15 ± 5 ($n = 3$), which is well above the limit of quantitation (LOQ, S/N of 9; Table S3). These data show that it is possible to monitor the enantioselective conversion of a few hundred cells in a nanoliter-sized reaction channel, even though the activity of ANEH (Table S4) and its expression in *E. coli* (Figure S8) are very low. As only a small portion of this reaction volume is transferred to the electrophoresis channel, further downsizing of the reaction volume appears feasible.

After successfully establishing an integrated chip device to follow enantioselective bioconversions by a countable number of cells, we applied the setup to study the on-chip reaction using ANEH-LW202 (Figure S9), an (S)-selective enzyme mutant previously engineered by directed evolution.¹⁶ This variant enabled a biotransformation with significantly improved enantiomeric excess (ee = 95%) and enhanced selectivity factor ($E \approx 100$ in favor of (S)-2).¹⁶ ANEH-LW202 was expressed in *E. coli*, and the cells were applied together with substrate 1 onto the microfluidic chip for 180 s as described above followed by MCE separation (Figure S9), resulting in an ee-value for (S)-2 of 93% and an E -value of 71 (Table 1). There were no differences in

Table 1. Calculated ee- and E -Values¹⁷ for Product 2 Formed upon Hydrolysis of Substrate 1 by Lysates and Whole Cells of *E. coli* Expressing ANEH-WT or LW202 on the Microfluidic Chip^a

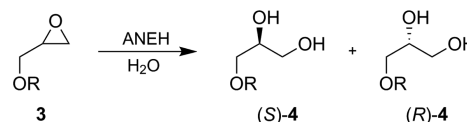
<i>E. coli</i>	ee/%		E	
	WT	LW202	WT	LW202
lysate	16 ± 8	95 ± 1	1.9 ± 0.4	81 ± 16
whole cell	13 ± 4	93 ± 1	1.7 ± 0.2	71 ± 15

^aThe values represent averages with standard deviation ($n = 3$).

ee-values (95 vs 93%), but the E -values (71 vs ~ 100) differed between the previous and current setup. To investigate if the difference was due to the new setup, we lysed the cells and performed the reaction with 1 (Figure S10). This resulted in a slightly higher E -value of 81 (ee-value of 95%), indicating that the selectivity is not affected but only conversion, possibly due to a lower reaction time or limited substrate diffusion by the cell membrane.¹⁸

To explore the versatility of the chip system, we analyzed various substrates that, e.g., serve as precursors of therapeutic agents:¹⁹ 2-[(3-methylphenoxy)methyl]oxirane (3a), glycidyl-4-methoxyphenyl-ether (3b), 4-chlorophenyl-glycidyl-ether (3c), and [(4-fluorophenoxy)methyl]oxirane (3d) (Scheme 2

Scheme 2. Enantioselective Hydrolysis of Oxiranylmethoxy Derivates



and Figure S11). *E. coli* expressing ANEH-WT displays no or low enantioselectivity of 3a, 3b, 3c and 3d (ee = -0.3 – 36% and $E = 0$ – 2.5), whereas ANEH-LW202 shows high enantioselectivity with ee-values of 81–95% and E -values of 12–95, respectively (Table 2). The E -values for 3a and 3b of 0 and 1.5 for ANEH-

Table 2. Calculated ee- and E -Values for Products 4 Formed upon Hydrolysis of Substrates 3 by *E. coli* Cells Expressing ANEH-WT or LW202 on the Microfluidic Chip^a

R	ee/%		E	
	WT	LW202	WT	LW202
4a ^b 3-CH ₃ C ₆ H ₄	-0.3 ± 0.7	81 ± 5	–	12 ± 4
4b ^b 4-OCH ₃ C ₆ H ₄	9 ± 1	93 ± 2	1.5 ± 0.1	41 ± 14
4c ^c 4-ClC ₆ H ₄	36 ± 12	92 ± 1	2.5 ± 0.7	40 ± 7
4d ^c 4-FC ₆ H ₄	26 ± 3	95 ± 2	2.1 ± 0.2	95 ± 54

^aThe values represent averages with standard deviation ($n = 3$). ^bThe catalytic hydrolyses of 3a and 3b are (S)-selective.^{16a,c} ^cAbsolute configurations of 4c and 4d not determined.¹⁹

WT as well as 12 and 41 for ANEH-LW202 were lower compared to 4 and 6 for ANEH-WT as well as 31 and 60 for ANEH-LW202 in the previous system, respectively.¹⁶ As mentioned above, the differences in E -values possibly arise from the short reaction times (180 s). As for 3c and 3d, these are the first examples of such biotransformations.

A main challenge in this study is the rather low fluorescence of the small aromatic analytes compared to bright fluorescent dyes commonly used in bioanalytics and single-cell studies. A significant step to circumvent this problem would be the use of more sensitive detection techniques for small molecules like mass spectrometry, which shows considerably higher detection performance compared to deep UV-fluorescence detection.²⁰ To monitor enantioselective catalysis at single cell or single particle level, it would be necessary to use confined picoliter sized reaction containers such as droplets²¹ or isolated microcavities²² which have recently been introduced for biochemical single-cell studies.

In conclusion, we analyzed various enantioselective reactions using only a few to several hundred cells with unaltered true enantiomeric substrates (not surrogates) in a minimized volume of 6.2 nL with an integrated and versatile chip device. Taking into account that the analyzed volume is only 50 pL, the study of single-cell catalysis appears to be within reach. In future work, we envision the usage of reaction volumes in picoliter dimension combined with next-generation protein expression systems to reach the goal of analyzing enantioselective reactions at the single-cell level for applications in high-throughput directed evolution and biocatalysis.

■ ASSOCIATED CONTENT

S Supporting Information

The Supporting Information is available free of charge on the ACS Publications website at DOI: 10.1021/jacs.5b12443.

Materials, microbiology and molecular biology details, experimental setups, signal assignment, limits of detection and quantitation, on-chip reaction data (PDF)

■ AUTHOR INFORMATION

Corresponding Authors

*belder@uni-leipzig.de

*reetz@mpi-muelheim.mpg.de

Notes

The authors declare no competing financial interest.

■ ACKNOWLEDGMENTS

K.M.K., R.W. and D.B. thank the Deutsche Forschungsgemeinschaft for funding. M.T.R. acknowledges the support of the LOEWE Research cluster (SynChemBio) of the state of Hessen, Germany.

■ REFERENCES

- (1) (a) Manz, A.; Graber, N.; Widmer, H. *Sens. Actuators, B* **1990**, *1*, 244–248. (b) Whitesides, G. M. *Nature* **2006**, *442*, 368–373. (c) Arora, A.; Simone, G.; Salieb-Beugelaar, G. B.; Kim, J. T.; Manz, A. *Anal. Chem.* **2010**, *82*, 4830–4847. (d) Mark, D.; Haerberle, S.; Roth, G.; von Stetten, F.; Zengerle, R. *Chem. Soc. Rev.* **2010**, *39*, 1153–1182.
- (2) (a) Ohno, K.; Tachikawa, K.; Manz, A. *Electrophoresis* **2008**, *29*, 4443–4453. (b) Culbertson, C. T.; Mickleburgh, T. G.; Stewart-James, S. A.; Sellens, K. A.; Pressnall, M. *Anal. Chem.* **2014**, *86*, 95–118.
- (3) (a) Dittrich, P. S.; Manz, A. *Nat. Rev. Drug Discovery* **2006**, *5*, 210–218. (b) Janasek, D.; Franzke, J.; Manz, A. *Nature* **2006**, *442*, 374–380. (c) Belder, D. *Angew. Chem., Int. Ed.* **2009**, *48*, 3736–3737. (d) Monošik, R.; Angnes, L. *Microchem. J.* **2015**, *119*, 159–168.
- (4) (a) Gomez, F. A. *Bioanalysis* **2010**, *2*, 1661–1662. (b) Yeo, L. Y.; Chang, H.-C.; Chan, P. P. Y.; Friend, J. R. *Small* **2011**, *7*, 12–48. (c) Bolivar, J. M.; Wiesbauer, J.; Nidetzky, B. *Trends Biotechnol.* **2011**, *29*, 333–342. (d) Araz, M. K.; Tentori, A. M.; Herr, A. E. *J. Lab. Autom.* **2013**, *18*, 350–366. (e) Chao, T.-C.; Hansmeier, N. *Proteomics* **2013**, *13*, 467–479. (f) Benz, C.; Retzbach, H.; Nagl, S.; Belder, D. *Lab Chip* **2013**, *13*, 2808–2814. (g) Li, X.; Xiao, D.; Ou, X.-M.; McCullm, C.; Liu, Y.-M. *J. Chromatogr. A* **2013**, *1318*, 251–256.
- (5) (a) Ispas, C. R.; Crivat, G.; Andreescu, S. *Anal. Lett.* **2012**, *45*, 168–186. (b) Shang, F.; Guihen, E.; Glennon, J. D. *Electrophoresis* **2012**, *33*, 105–116. (c) Gomez, F. A. *Bioanalysis* **2013**, *5*, 1–3.
- (6) (a) Dittrich, P. S.; Manz, A. *Anal. Bioanal. Chem.* **2005**, *382*, 1771–1782. (b) Götz, S.; Karst, U. *Anal. Bioanal. Chem.* **2006**, *387*, 183–192. (c) Mogensen, K. B.; Kutter, J. P. *Electrophoresis* **2009**, *30*, S92–S100. (d) Li, Q.; Seeger, S. *Appl. Spectrosc. Rev.* **2010**, *45*, 12–43.
- (7) (a) deMello, A. J. *Nature* **2006**, *442*, 394–402. (b) Brivio, M.; Verboom, W.; Reinhoudt, D. N. *Lab Chip* **2006**, *6*, 329–344. (c) Wiles, C.; Watts, P. *Chem. Commun.* **2011**, *47*, 6512. (d) Rodrigues, T.; Schneider, P.; Schneider, G. *Angew. Chem., Int. Ed.* **2014**, *53*, S750–S758. (e) McQuade, D. T.; Seeberger, P. H. *J. Org. Chem.* **2013**, *78*, 6384–6389. (f) Trapp, O.; Weber, S. K.; Bauch, S.; Hofstadt, W. *Angew. Chem., Int. Ed.* **2007**, *46*, 7307–7310. (g) Benz, C.; Boomhoff, M.; Appun, J.; Schneider, C.; Belder, D. *Angew. Chem., Int. Ed.* **2015**, *54*, 2766–2770.
- (8) (a) Fritzsche, S.; Ohla, S.; Glaser, P.; Giera, D. S.; Sickert, M.; Schneider, C.; Belder, D. *Angew. Chem., Int. Ed.* **2011**, *50*, 9467–9470. (b) Troendlin, J.; Rehbein, J.; Hiersemann, M.; Trapp, O. *J. Am. Chem. Soc.* **2011**, *133*, 16444–16450. (c) Ohla, S.; Beyreiss, R.; Fritzsche, S.; Gläser, P.; Nagl, S.; Stockhausen, K.; Schneider, C.; Belder, D. *Chem. - Eur. J.* **2012**, *18*, 1240–1246. (d) Stockinger, S.; Troendlin, J.; Rominger, F.; Trapp, O. *Adv. Synth. Catal.* **2015**, *357*, 3513–3520.
- (9) Belder, D.; Ludwig, M.; Wang, L. W.; Reetz, M. T. *Angew. Chem., Int. Ed.* **2006**, *45*, 2463–2466.
- (10) (a) Piehl, N.; Ludwig, M.; Belder, D. *Electrophoresis* **2004**, *25*, 3848–3852. (b) Nagl, S.; Schulze, P.; Ludwig, M.; Belder, D. *Electrophoresis* **2009**, *30*, 2765–2772. (c) Preinerstorfer, B.; Lämmerhofer, M.; Lindner, W. *Electrophoresis* **2009**, *30*, 100–132. (d) Nagl, S.; Schulze, P.; Ohla, S.; Beyreiss, R.; Gitlin, L.; Belder, D. *Anal. Chem.* **2011**, *83*, 3232–3238. (e) Scriba, G. K. E. *J. Sep. Sci.* **2008**, *31*, 1991–2011.
- (11) (a) de Carvalho, C. C. R. *Biotechnol. Adv.* **2011**, *29*, 75–83. (b) Schrewe, M.; Julsing, M. K.; Bühler, B.; Schmid, A. *Chem. Soc. Rev.* **2013**, *42*, 6346–6377.
- (12) (a) Bommarius, A. S. *Annu. Rev. Chem. Biomol. Eng.* **2015**, *6*, 319–345. (b) Gillam, E. M. J.; Copp, J. N.; Ackerley, D. F. *Methods Mol. Biol.*; Humana Press: Totowa, 2014. (c) Reetz, M. T. *Directed Evolution of Enzymes*. In *Enzyme Catalysis in Organic Synthesis*, 3rd ed.; Drauz, K.; Gröger, H.; May, O., Ed.; Wiley-VCH: Weinheim, 2012; Vol. 1, pp 119–190. (d) Jäckel, C.; Hilvert, D. *Curr. Opin. Biotechnol.* **2010**, *21*, 753–759. (e) Brustad, E. M.; Arnold, F. H. *Curr. Opin. Chem. Biol.* **2011**, *15*, 201–210. (f) Goldsmith, M.; Tawfik, D. S. *Curr. Opin. Struct. Biol.* **2012**, *22*, 406–412. (g) Widersten, M. *Curr. Opin. Chem. Biol.* **2014**, *21*, 42–47. (h) Denard, C. A.; Ren, H.; Zhao, H. *Curr. Opin. Chem. Biol.* **2015**, *25*, 55–64. (i) Currin, A.; Swainston, N.; Day, P. J.; Kell, D. B. *Chem. Soc. Rev.* **2015**, *44*, 1172–1239. (j) Turner, N. J. *Nat. Chem. Biol.* **2009**, *5*, S67–S73. (k) Siloto, R. M. P.; Weselake, R. J. *Biocatal. Agric. Biotechnol.* **2012**, *1*, 181–189. (l) Lutz, S.; Bornscheuer, U. T. *Protein Engineering Handbook*; Wiley-VCH: Weinheim, 2009.
- (13) (a) Colin, P.-Y.; Zinchenko, A.; Hollfelder, F. *Curr. Opin. Struct. Biol.* **2015**, *33*, 42–51. (b) Kintsjes, B.; van Vliet, L. D.; Devenish, S. R. A.; Hollfelder, F. *Curr. Opin. Chem. Biol.* **2010**, *14*, 548–555. (c) Taly, V.; Kelly, B. T.; Griffiths, A. D. *ChemBioChem* **2007**, *8*, 263–272. (d) Kelly, B. T.; Baret, J.-C.; Taly, V.; Griffiths, A. D. *Chem. Commun.* **2007**, 1773–1788.
- (14) Acevedo-Rocha, C. G.; Agudo, R.; Reetz, M. T. *J. Biotechnol.* **2014**, *191*, 3–10.
- (15) Becker, S.; Höbenreich, H.; Vogel, A.; Knorr, J.; Wilhelm, S.; Rosenau, F.; Jaeger, K.-E.; Reetz, M. T.; Kolmar, H. *Angew. Chem., Int. Ed.* **2008**, *47*, 5085–5088.
- (16) (a) Wang, L.-W. Ph.D. Dissertation, Ruhr-Universität Bochum, Germany, 2006. (b) Reetz, M. T.; Wang, L. W.; Bocola, M. *Angew. Chem., Int. Ed.* **2006**, *45*, 1236–1241. (c) Reetz, M. T.; Bocola, M.; Wang, L.-W.; Sanchis, J.; Cronin, A.; Arand, M.; Zou, J.; Archelas, A.; Bottalla, A.-L.; Naworyta, A.; Mowbray, S. L. *J. Am. Chem. Soc.* **2009**, *131*, 7334–7343.
- (17) Faber, K. *Biotransformations in Organic Chemistry*; Springer-Verlag: Berlin, 2004; pp 40–43.
- (18) Kang, D. G.; Li, L.; Ha, J. H.; Choi, S. S.; Cha, H. J. *Korean J. Chem. Eng.* **2008**, *25*, 804–807.
- (19) (a) Truscillo, A. M.; Gambarotti, C.; Lauria, M.; Auricchio, S.; Leonardi, G.; Shisodia, S. U.; Citterio, A. *Green Chem.* **2013**, *15*, 625–628. (b) Phillips, E. D.; Chang, H.-F.; Holmquist, C. R.; McCauley, J. P. *Bioorg. Med. Chem. Lett.* **2003**, *13*, 3223–3226.
- (20) (a) Schwarzkopf, F.; Scholl, T.; Ohla, S.; Belder, D. *Electrophoresis* **2014**, *35*, 1880–1886. (b) Beyreiss, R.; Geißler, D.; Ohla, S.; Nagl, S.; Posch, T. N.; Belder, D. *Anal. Chem.* **2013**, *85*, 8150–8157.
- (21) (a) Joansson, H. N.; Andersson Svahn, H. *Angew. Chem., Int. Ed.* **2012**, *51*, 12176–12192. (b) Lagus, T. P.; Edd, J. F. *J. Phys. D: Appl. Phys.* **2013**, *46*, 114005–1–21. (c) Song, H.; Chen, D. L.; Ismagilov, R. F. *Angew. Chem., Int. Ed.* **2006**, *45*, 7336–7356.
- (22) (a) Stratz, S.; Eyer, K.; Kurth, F.; Dittrich, P. S. *Anal. Chem.* **2014**, *86*, 12375–12381. (b) Eyer, K.; Stratz, S.; Kuhn, P.; Küster, S. K.; Dittrich, P. S. *Anal. Chem.* **2013**, *85*, 3280–3287. (c) Eyer, K.; Kuhn, P.; Hanke, C.; Dittrich, P. S. *Lab Chip* **2012**, *12*, 765–772.